AD-A184 471 NUMERICAL STUDIES OF THE DUAL HEMT/ALGORITHM DEVELOPMENT AND NUMERICAL ST (U) SCIENTIFIC RESEARCH ASSOCIATES INC GLASTONBURY CT H L GRUBIN ET AL 1/1

UNCLASSIFIED 03 AUG 87 SRA-R930012F ARO-23398 1-EL-5 F/G 9/1 NL

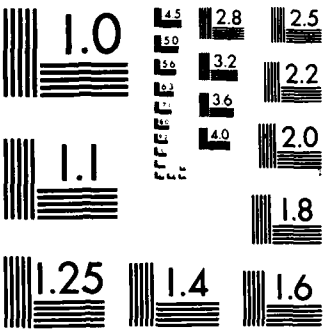

ARO 23398.1-EL-S

(2)

NUMERICAL STUDIES OF THE DUAL HEMT/ALGORITHM DEVELOPMENT AND NUMERICAL STUDIES OF SCHRODINGER'S EQUATION

SRA FINAL REPORT R930012F

H.L.GRUBIN
M.MEYYAPPAN
J.P.KRESKOVSKY
S.M.PINCUS

AUGUST 1987

U.S. ARMY RESEARCH OFFICE

CONTRACT NUMBER DAAL03-86-C-0013

SCIENTIFIC RESEARCH ASSOCIATES, INC.
P.O.BOX 1058
GLASTONBURY, CONNECTICUT 06033

UNCLASSIFIED
SECURITY CLASSIFICATION OF THIS PAGE

REPORT DOCUMENTATION PAGE

1a. REPORT SECURITY CLASSIFICATION: Unclassified	1b. RESTRICTIVE MARKINGS
2a. SECURITY CLASSIFICATION AUTHORITY	3. DISTRIBUTION/AVAILABILITY OF REPORT: Approved for public release; distribution unlimited.
2b. DECLASSIFICATION/DOWNGRADING SCHEDULE	
4. PERFORMING ORGANIZATION REPORT NUMBER(S)	5. MONITORING ORGANIZATION REPORT NUMBER(S)
6a. NAME OF PERFORMING ORGANIZATION: Scientific Research Associates; 6b. OFFICE SYMBOL (If applicable)	7a. NAME OF MONITORING ORGANIZATION: U. S. Army Research Office
6c. ADDRESS (City, State, and ZIP Code): P.O. Box 1058, Glastonbury, CT 06033	7b. ADDRESS (City, State, and ZIP Code): P. O. Box 12211, Research Triangle Park, NC 27709-2211
8a. NAME OF FUNDING/SPONSORING ORGANIZATION: U. S. Army Research Office; 8b. OFFICE SYMBOL (If applicable)	9. PROCUREMENT INSTRUMENT IDENTIFICATION NUMBER: DAAL03-86-C-0013
8c. ADDRESS (City, State, and ZIP Code): P. O. Box 12211, Research Triangle Park, NC 27709-2211	10. SOURCE OF FUNDING NUMBERS: PROGRAM ELEMENT NO. / PROJECT NO. / TASK NO. / WORK UNIT ACCESSION NO.

11. TITLE (Include Security Classification)
Numerical Studies of the Dual HEMT/Algorithm Development and Numerical Studies of Schrodinger's Equation

12. PERSONAL AUTHOR(S)
H.L. Grubin, M. Meyyappan, J.P. Kreskovsky, S.M. Pincus

13a. TYPE OF REPORT	13b. TIME COVERED	14. DATE OF REPORT (Year, Month, Day)	15. PAGE COUNT
Final Report	FROM 15Apr86 TO 14Apr87	1987 August 3	- 17 -

16. SUPPLEMENTARY NOTATION
The view, opinions and/or findings contained in this report are those of the author(s) and should not be construed as an official Department of the Army position, policy, or decision, unless so designated by other documentation.

17. COSATI CODES		
FIELD	GROUP	SUB-GROUP

18. SUBJECT TERMS (Continue on reverse if necessary and identify by block number)
Dual HEMT, AlGaAs, GaAs Switching Times, Numerical Simulations, Schrodinger's Equation

19. ABSTRACT (Continue on reverse if necessary and identify by block number)
This document describes work carried out, at Scientific Research Associates, Inc., of Glastonbury, Connecticut (SRA), under Contract DAAL03-86-C-0013 for the period 15 April 1986 to 14 April 1987. Two studies were initiated under this Contract. One study was concerned with establishing a set of design procedures for the dual HEMT. The second was to develop algorithms and examine transport in quantum based electronic devices.

20. DISTRIBUTION/AVAILABILITY OF ABSTRACT	21. ABSTRACT SECURITY CLASSIFICATION
☐ UNCLASSIFIED/UNLIMITED ☐ SAME AS RPT. ☐ DTIC USERS	Unclassified
22a. NAME OF RESPONSIBLE INDIVIDUAL	22b. TELEPHONE (Include Area Code) / 22c. OFFICE SYMBOL

DD FORM 1473, 84 MAR — 83 APR edition may be used until exhausted. All other editions are obsolete.

SECURITY CLASSIFICATION OF THIS PAGE
UNCLASSIFIED

NUMERICAL STUDIES OF THE DUAL HEMT/ ALGORITHM DEVELOPMENT AND NUMERICAL STUDIES OF SCHRODINGER'S EQUATION

INTRODUCTION

This document describes work carried out, at Scientific Research Associates, Inc. of Glastonbury, Connecticut (SRA), under Contract DAAL03-86-C-0013 for the period 15 April 1986 to 14 April 1987.

Two studies were *initiated* under this Contract. It is anticipated that both studies will be included in broader programs under development. One study was concerned with establishing a set of design procedures for the dual HEMT. The second was to develop algorithms and examine transport in quantum based electronic devices. The results of the latter study are currently being incorporated into other programs underway at SRA. Insofar as both studies are in their early stages, they will be only briefly described. The dual HEMT is considered first.

DUAL HEMT STUDIES

The dual HEMT structure, as originally proposed, is shown in Fig. 1. It consists of an ordinary HEMT structure with three terminals sitting on top of an AlGaAs semi-insulating substrate. Secondary source and drain contacts are added to the semi-insulating GaAs. One objective in the design of this device was that it would be a superior switching device device with regard to *switching times*. Here it was thought that the switching time would be governed by the time it took for the depletion layer of the device to move from its quiescent state to the bottom of the channel. Earlier work performed by the Principal Investigator on switching times on GaAs and silicon FETs indicated that only a small fraction of the total switching time was involved in moving the depletion region from one region of the device to another. A longer fraction of time was spent discharging the excess charge through the

source and drain contact. This latter result was also obtained by workers at the University of Illinois, who examined a symmetric dual HEMT. In the present SRA study, switching times were not studied. Rather, *the initial SRA program concentrated on determining the distribution of charge within the device and the subsequent control that might be exercised through biasing constraints. It is anticipated that switching time studies will form the basis of future programs.*

One operational form for this device was that the device could operate in two modes. One is the standard HEMT mode. The second and more interesting mode involves reverse biasing the gate to values in which the depletion layer moves to the semi-insulating AlGaAs region. Thus HEMT transport in eliminated and secondary transport initiated. It must be remarked at this point, that the configuration for studying this proposal was not necessarily optimum. For example, contacts and subsequent transport through semi-insulating GaAs is a topic of its own. Rather, proof of principle of operation was sought.

To examine this problem the semiconducting drift and diffusion equations were solved. These equations included Poisson's equation, and the equation of continuity for electrons and holes. For heterostructures, the equations of current flow for electrons and holes is best expressed as,

$$Jn = \mu kT[\nabla(\hat{E}_C/kT) + \nabla n] \tag{1}$$

$$J_p = \mu kT[\nabla(\hat{E}_V/kT) + \nabla p] \tag{2}$$

$$\hat{E}_C = E(x) - \chi - kT\ln n_C \tag{3}$$

$$\hat{E}_V(x) = + E(x) - \chi(x) - Eg + kT\ln n_V(x) \tag{4}$$

where E(x) is the electrostatic energy of the carriers as obtained from Poisson's equation, $n_c(x)$, $n_v(x)$, are the conduction and valence band

density of states, respectively, and χ is the electron affinity.

Numerical solution to the governing equations requires specification of the carrier density on the contacts, the electrostatic energy on the boundaries, and, in our case, a condition of zero current flow across noncontacted exposed surfaces. A typical procedure for solving these problems is to determine the built-in potential for the zero current quiescent solution and then to subtract the built-in potential from all subsequent solutions. Thus all subsequent solutions describe departures from equilibrium. In one dimension, the built-in potential may be obtained as a solution to equation (1) for zero current and is obtained implicitly from

$$n(x) = \exp-[\hat{E}_C(x) - E_F]/kT \tag{5}$$

Thus if the carrier density at the contacts is know, the electrostatic energy at the contacts are known, and the zero applied bias built-in potential can be determined. The numerical implementation of this procedure is, in principle, direct, but it's success is often dependent upon the field variations within the vicinity of the boundaries. In particular, long contacted boundary regions offer the most success.

For the dual HEMT the bias levels of individual contacts was varied until the net current flow between the contacts was below a prespecified value. These bias levels were the empirically determined built in potentials, and all other potentials are discussed with reference to them.

Eleven calculations were performed for the structure of figure 1, using the grid of figure 2. The convention for these calculations is that negative source and drain current signifies current *into* the device. Positive source and drain current denotes current *out of* the device. Figure 3 displays the primary and secondary source currents as a function of bias. Figure 4 displays the same for the drain contacts.
For these figures, eleven calculations were performed. The gate bias levels are indicated in the insert. The relative source and drain currents are

indicated in the accompanying charts. Note, for the source contacts, *all current are into the device*, but the relative magnitudes of the current are bias dependent. Only for calculations "9" and "10" were the primary and secondary source currents equal; the drain currents were not equal.

The details of the #"9" calculation are considered in more detail in the accompanying figures. Figure 5 displays the distribution of total current into and out of the contacts, as well as the specific dimensions of the structure. Figure 6 displays the distribution of charge normal to the gate along line of symmetry. Figure 7 displays the potential contours for this calculation. Figure 8 displays the current streamlines. The important point to note here is that there is a significant charge distribution within the AlGaAs layer, and it is within this layer that most of the current is flowing. Thus for calculation "9" most of the charge that reaches the region under the gate, behaves as "HEMT" charge. The distribution of charge and current within the contact regions is another matter. For example, figure 9 displays the current streamlines within the regions near, the source contacts, the drain contacts, and the region under the gate. The important points to note here is that there are circulating currents within the contact regions, but that "one-dimensional" transport appears to be occurring under the gate.

Our experience with these calculations indicates that while most of the current is flowing through the AlGaAs, the distribution of current into the structure is appears to be determined by the potential on the gate. Figure 10 illustrates the streamlines for the case of a strong reverse bias on the gate. These results suggest that is *at any given bias level the amount of current flowing in the device from the different source and drain contacts is controlled by the gate*.

While major control of the distribution of current was obtained by varying the gate bias, altering the primary and secondary source potentials also altered both the paths of current flow and their magnitudes. However, for the parameters of this calculation the most significant path alteration occurred with respect to the drain. Here, not only was the magnitude of the current altered, but the sign was changed. Thus current could be flowing in through

the drain contacts. All of these calculations led to the conclusion that the dual HEMT structure considered in figure 1 was significantly cross-talk dependent.

An unusual feature of this structure, is that the dimensions and doping of the device resulted in an operation in which the degree to which the source and drain contacts interacted was critically dependent upon the gate potential, and a suggestion of operation is that for certain value of gate bias levels, it may be possible to vary the local potentials on the primary and secondary source and drain contacts and have them operate independently of each other. Here cross-talk is the mode of operation.

Thus the initial calculations demonstrated that most of the current was flowing in the heavily-doped AlGaAs region, that there was no significant transport in the two-dimensional electron gas region, and that cross-talk was a major issue. Depleting the AlGaAs required strong reverse bias levels on the gate. To eliminate the latter problem problem, as well as to achieve a design that was closer to that being fabricated at Fort Monmouth, the structure shown in Fig. 11 was studied. Here only one calculation was performed. This calculation demonstrated that cross-talk was still present but that depletion of the channel would be easier.

The question that then arose was whether, on the basis of these calculations, we could determined how this device operates. While it is too early to obtain a complete determination of this answer, some preliminary conclusions can be drawn. For a bias that does not move the depletion region to the bottom of the semi-insulating gallium arsenide region, all four source and drain contacts will interact. For a sufficiently reverse bias, and for the dimensions and doping level implemented in the study of this device, it appears that the depleted region is capable of isolating the source contact regions from the drain contact regions, thus yielding separate "source" and "drain" region devices. Full operational physics of this device remains to be determined.

To eliminate cross-talk completely, it would be necessary to fabricate a

symmetric dual HEMT device in which the source and drain contacts of the primary and secondary metallizations are tied to each other, as is being done by the University of Illinois.

QUANTUM TRANSPORT STUDIES

In the area of quantum transport, most of the effort under the first phase of the study was to put in place, procedures for obtaining eigenvalues for a variety of different barriers and wells. Thus algorithms were developed and a number of model problems were investigated. These procedures are now in place. In addition, the time dependent Schrodinger equation was solved.

The time dependent Schrodinger equation was solved for single barriers and tunnel barriers. Insofar as some time dependent algorithms are inherently dissipative, particular emphasis was spent on developing a procedure that was not dissipative. Thus, the time dependent probability was computed for each run, and shown that for the duration of the run, its normalization was always unity. Typical structures for the calculation were 1200A in length, subject to fixed boundary conditions and an initial wave packet distribution. The boundary conditions permitted the variation of carrier density on the boundary. The variation of carrier density on the boundary did not result in any marked variation in the time dependent behavior of the wave packet. Indeed, one of the difficulties with the approach of examining transport in tunnel barriers with realistic boundaries, is the difficulty in implementing a suitable set of current boundary conditions. An alternative procedure was sought. As discussed in the proposal, the approach to be taken was from the moments of the density matrix. This procedure was initiated near the termination of the ARO study, and continued under another program. Initial calculations with this approach appears to be fruitful.

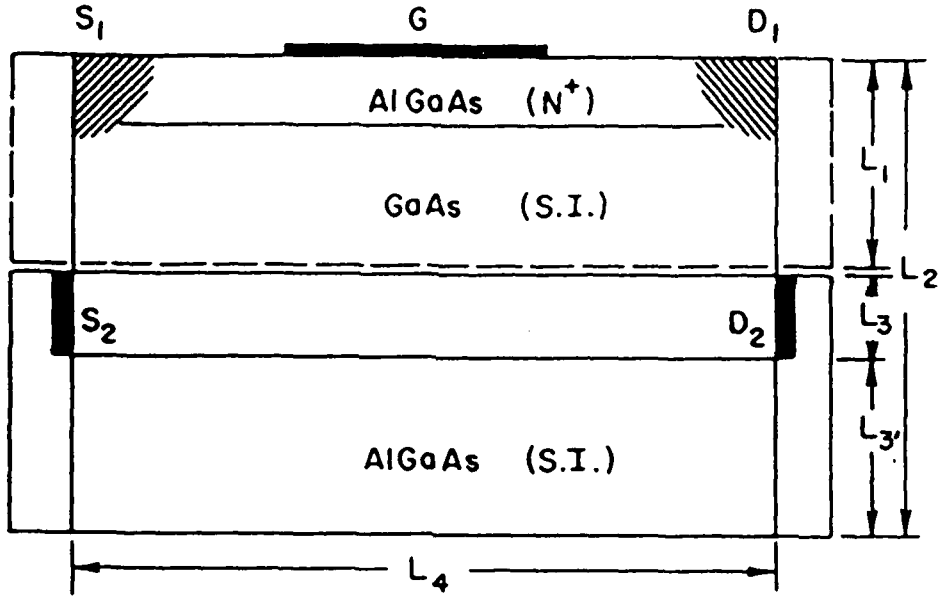

FIGURE 1. Schematic of the dual HEMT.

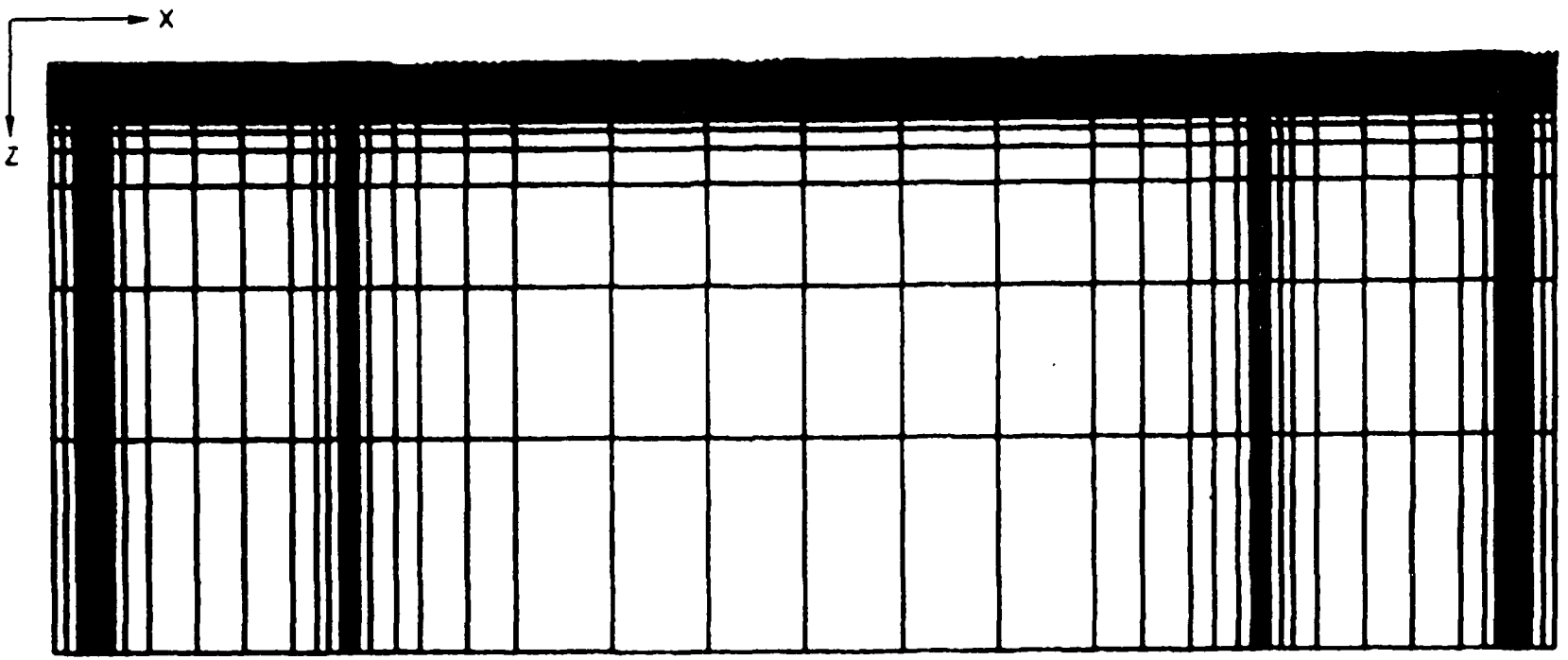

FIGURE 2. Grid structure used in the study.

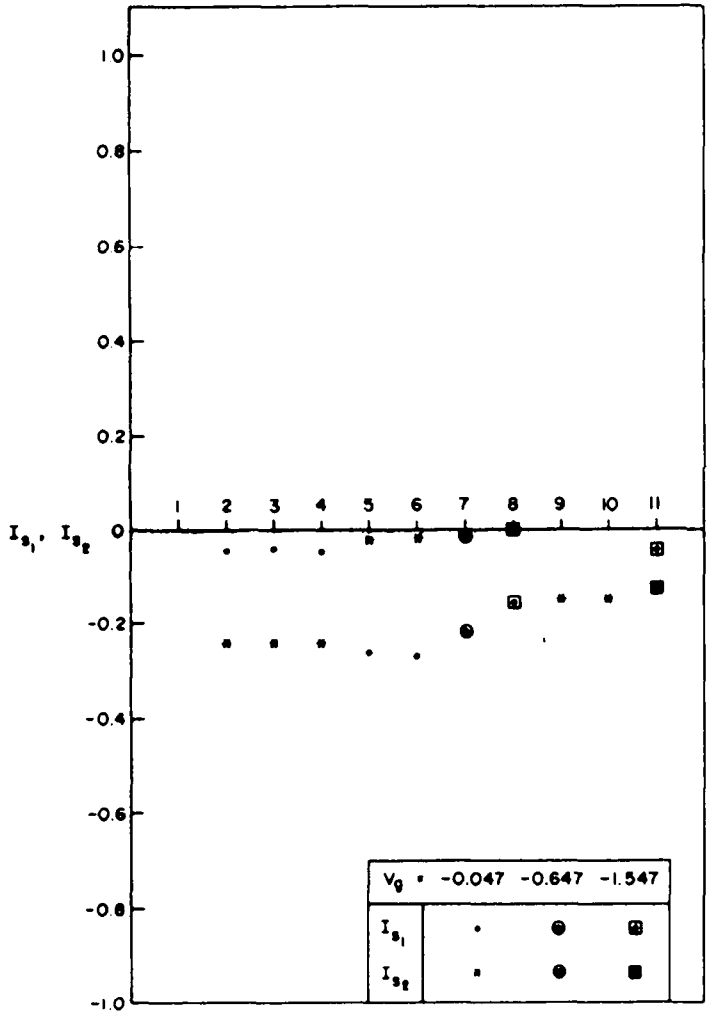

	$V_{S_2} - V_{S_1}$	$V_{D_2} - V_{D_2}$	$V_{D_2} - V_{S_1}$
2	-0.089	-2.089	0.0
3	-0.089	-1.589	0.5
4	-0.089	-0.089	2.0
5	0.089	-1.411	1.5
6	0.089	0.089	2.0
7	0.089	0.089	2.0
8	0.089	0.089	2.0
9	0.00	0.089	2.089
10	0.00	0.589	2.589
11	0.00	0.089	2.089

FIGURE 3. Primary and secondary source currents as a function of bias.

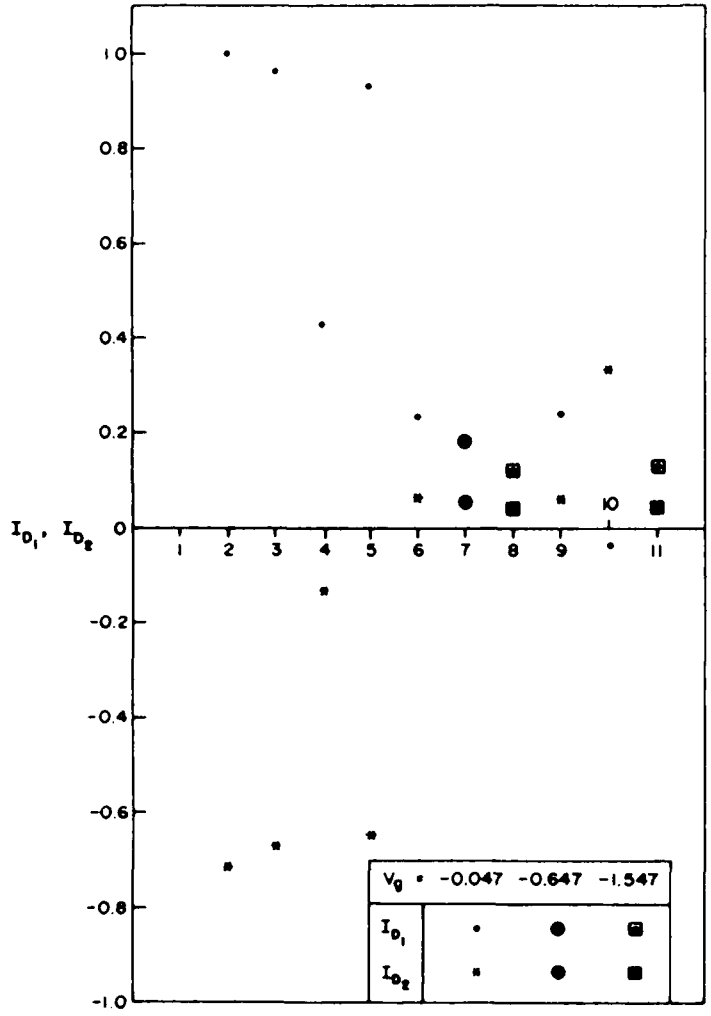

	$V_{S_2} - V_{S_1}$	$V_{D_2} - V_{D_2}$	$V_{D_2} - V_{S_1}$
2	-0.089	-2.089	0.0
3	-0.089	-1.589	0.5
4	-0.089	-0.089	2.0
5	0.089	-1.411	1.5
6	0.089	0.089	2.0
7	0.089	0.089	2.0
8	0.089	0.089	2.0
9	0.00	0.089	2.089
10	0.00	0.589	2.589
11	0.00	0.089	2.089

FIGURE 4. Primary and secondary drain currents as a function of bias.

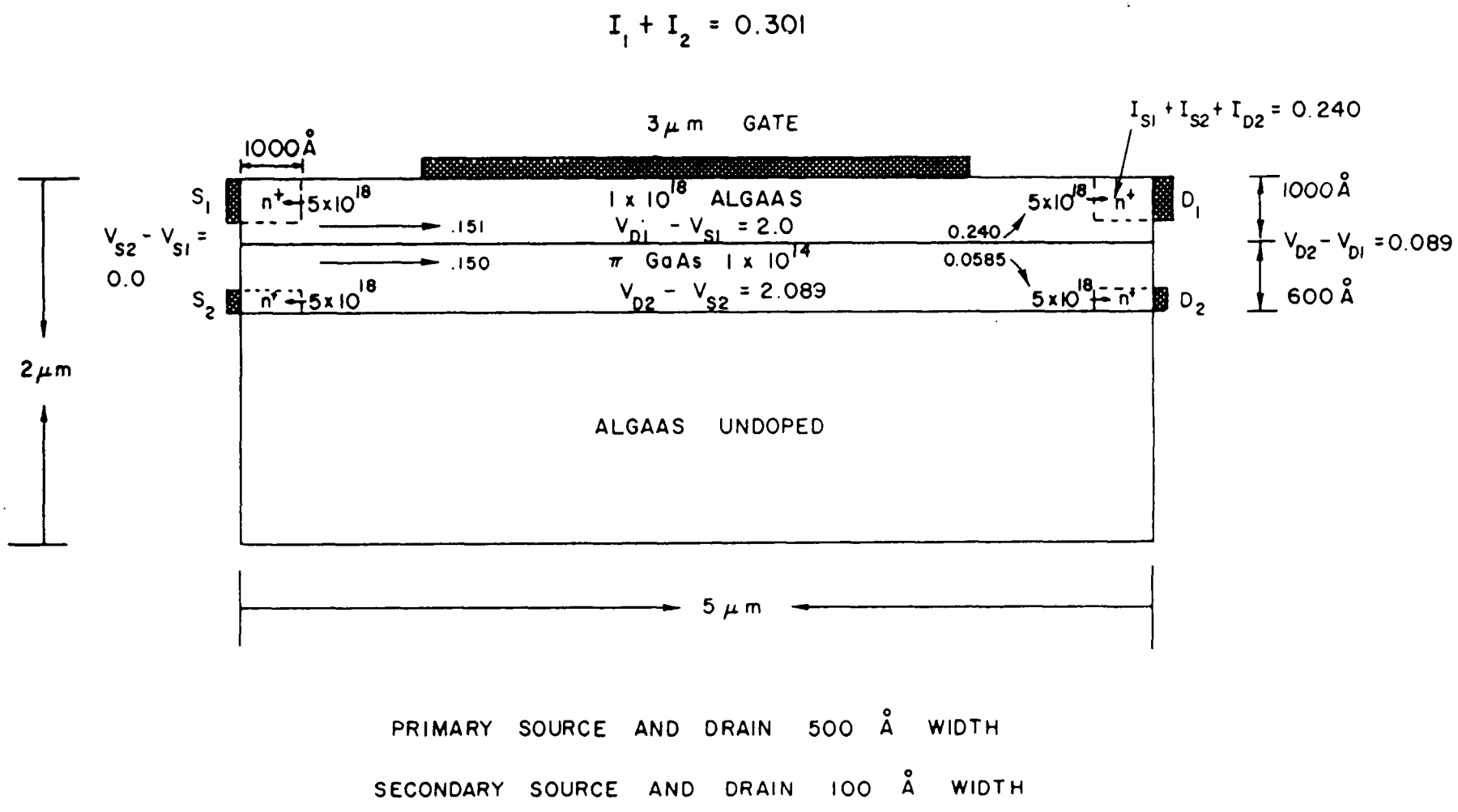

FIGURE 5. Dimensions of the structure studied as well as the distribution of current into and out of the device for calculation "9".

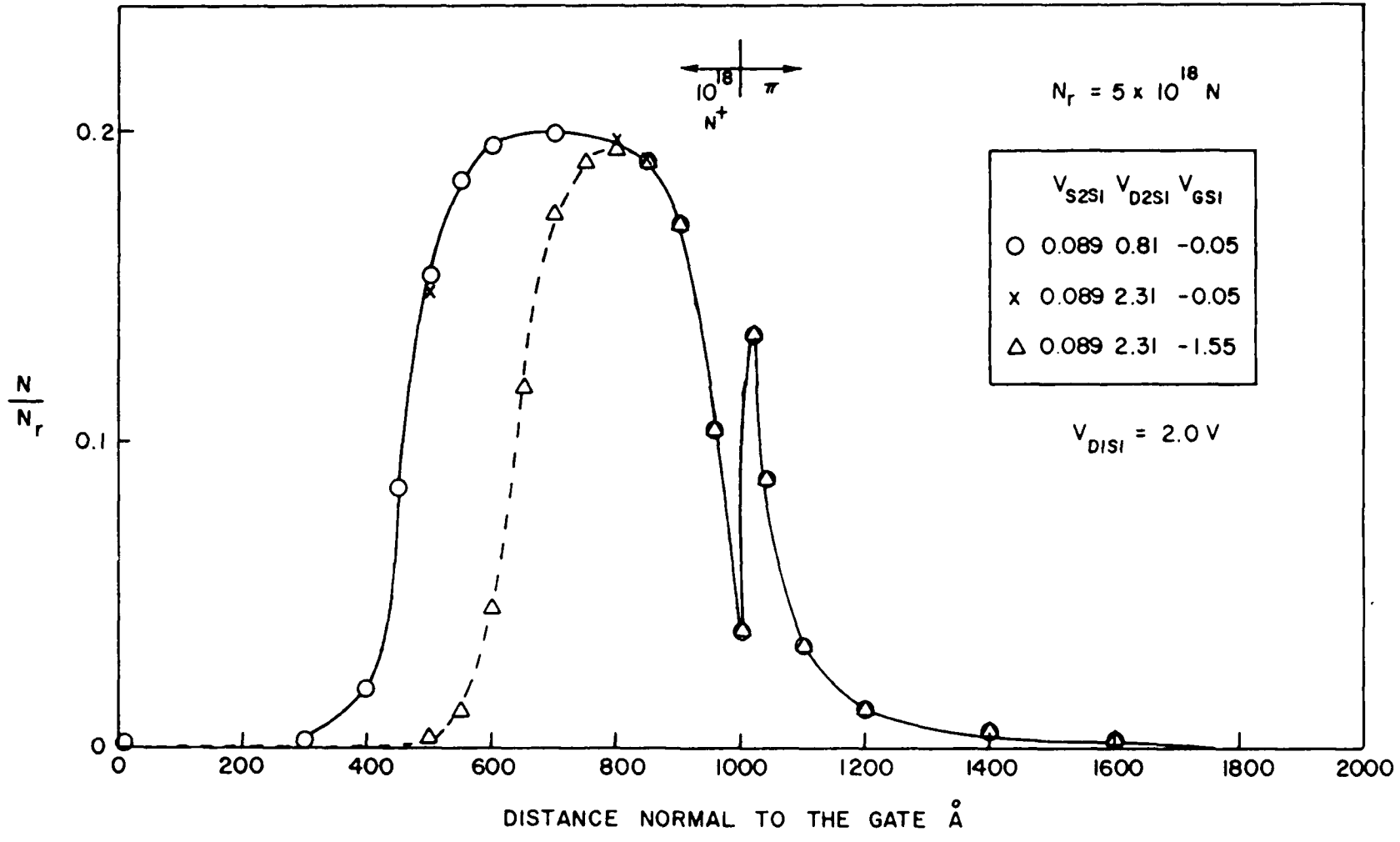

FIGURE 6. Distribution of charge normal to the gate along a line of symmetry, for different values of bias for calculation "9".

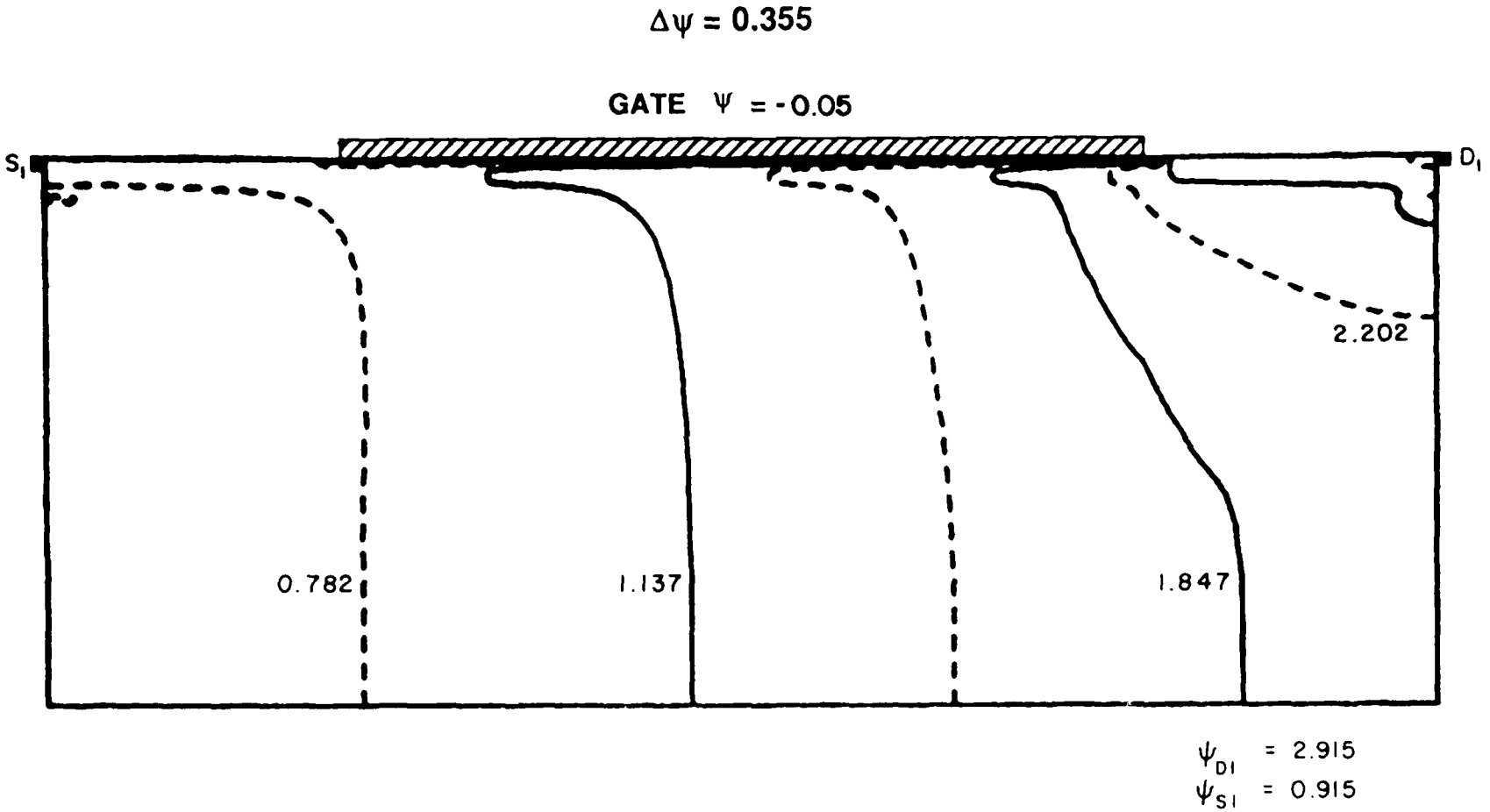

FIGURE 7. Potential contours for calculation "9".

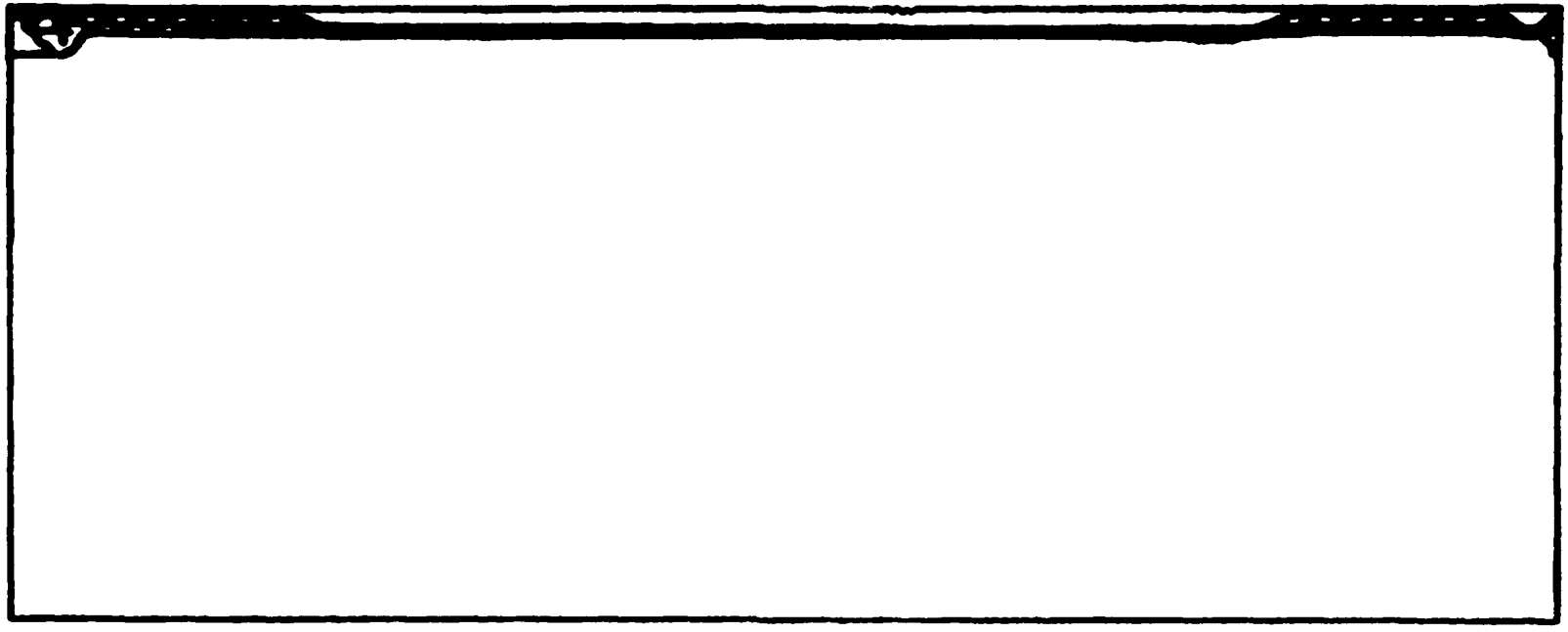

FIGURE 8. Current streamlines for calculation "9".

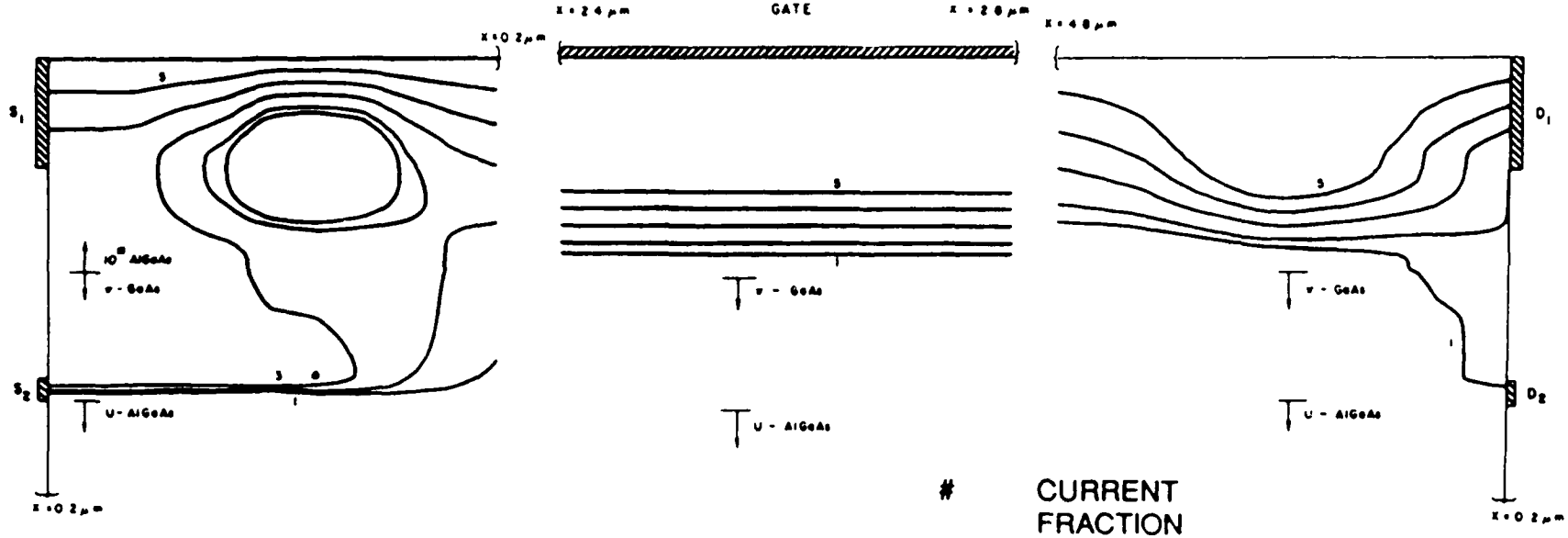

FIGURE 9. A blow-up of the current streamlines within the vicinity of the source contacts, the drain contacts and the region under the gate.

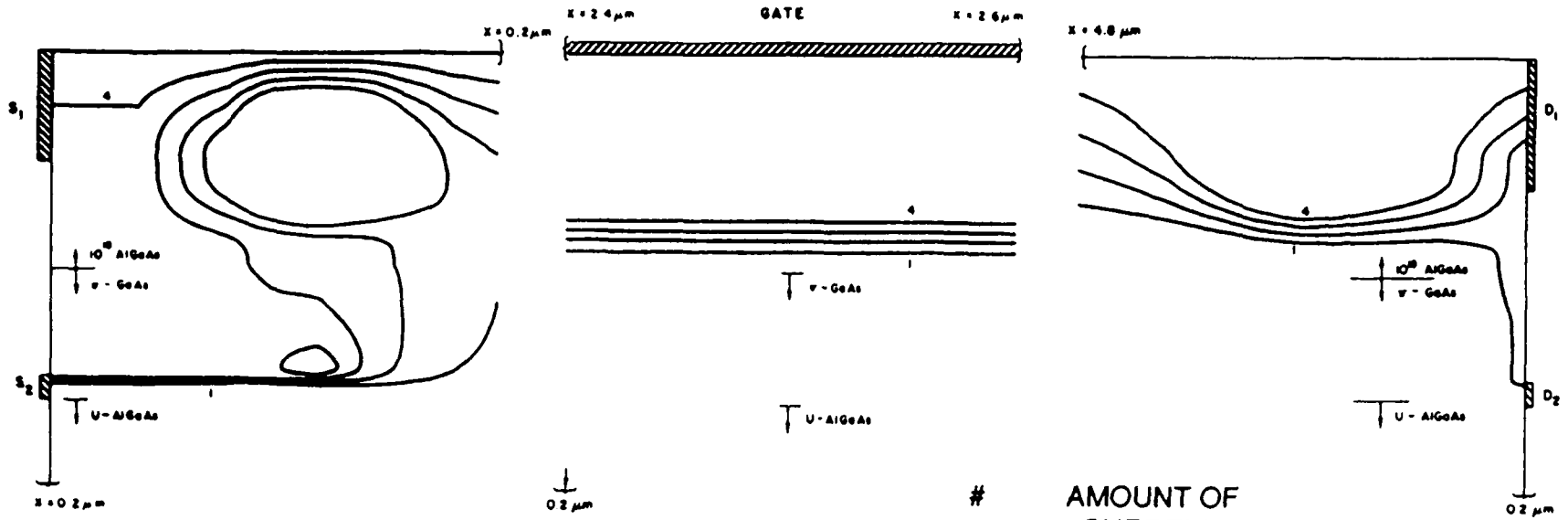

FIGURE 10. As in Fig. 9, but for a more negative bias on the gate.

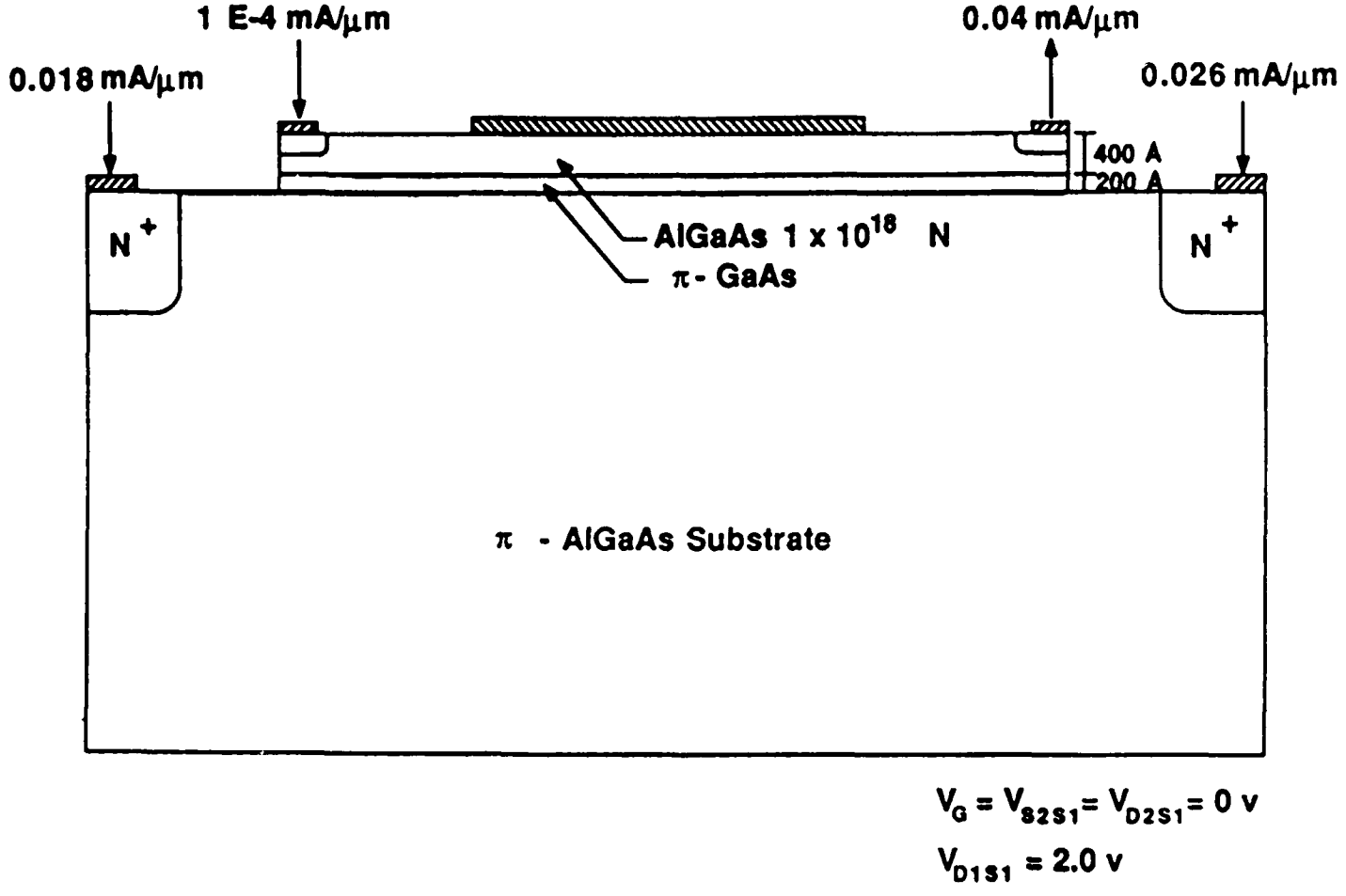

FIGURE 11. Second dual HEMT structure for which calculations were performed.

END

10-87

DTIC